Top of salt impact on full waveform inversion sediment velocity update

Kai (Ky) Wang, Bin Deng, Zhigang Zhang, Lingli Hu, Yan Huang, CGG*

Summary

Full waveform inversion (FWI) usually gives a poor update of the sediment velocity when in the close vicinity of the top of salt (TOS) reflection. This phenomenon is a common practical challenge and is due to the strong velocity contrast between the sediment and salt—although its exact cause is not yet well understood. We investigated the relationship between FWI's sediment velocity update and the role of salt insertion, namely the accuracy of the salt interface used in the FWI input velocity model. The results indicated that the initial model with salt inserted helps update the sediment model, and furthermore, using a more accurate TOS (i.e., the TOS interpretation used to insert the salt is closer to the true TOS) provides a better sediment velocity update. However, an accurate TOS is not available unless the sediment velocity, particularly directly above the TOS, has been correctly updated. Therefore, we propose a workflow to obtain a more accurate TOS for the FWI sediment velocity update using iterative FWI and salt interpretation. Using 2D synthetic data and 3D real data, we demonstrate that our workflow yields a better FWI update above the salt compared to using the sediment model as the initial model.

Introduction

FWI aims to minimize the misfit of phase and amplitude between real shot gathers and synthetic shot gathers (Lailly, 1983; Tarantola, 1984; Sirgue and Pratt, 2004; Virieux and Operto, 2009). Updating the velocity in areas of high impedence and/or velocity contrast, such as the sediment-salt boundary, is challenging for FWI. Two approaches are commonly used to address this overburden velocity update problem. Kapoor et al. (2012) used sediment models created from ray-tracing tomography as FWI input. Chen et al. (2014) used a salt model approach that ran an initial pass of FWI with the sediment model to update the sediment velocity before creating a salt model for the second pass of FWI to update the sediment velocity again. However, few studies have been performed to understand the impact of the TOS interpretation on the sediment velocity update using FWI. By using band limited data and conventional FWI, the TOS singularities are not automatically updated at each iteration.

If a sediment model is used as the FWI initial model, the reflections and refractions from the TOS, which are strong in amplitude, are absent in the synthetic shot gathers. This considerable mismatch in the data leads to artifacts along the TOS in the updated velocity model. Two solutions to this problem are either to mute the TOS events in the real data before FWI or to mute the incorrect velocity update right above the TOS in the model after FWI. However, it is difficult to only remove the events created by TOS in the shot domain, particularly at far offsets where the TOS reflections are often mixed with diving waves and refractions. By using a salt model as the FWI initial model, the synthetic data contains the TOS events that match the real data. However, an incorrect TOS interpretation due to an inaccurate supra-salt velocity or bad horizon picking may still cause an incorrect velocity update in the FWI. Inverting the location of the TOS and sediment velocity above the TOS at the same time remains challenging.

We compared FWI results using different initial models of sediment and salt with different magnitudes of errors in the TOS in respect to the true TOS. Based on these results, we created a workflow that uses the salt flood model as the initial model to update the sediment velocity with the FWI and then updates the TOS based on this updated sediment velocity. The salt flood model is then recreated with the initial sediment velocity and the updated TOS is used to run FWI again. The updated sediment velocity model is not used here because artifacts caused by the erroneous TOS may mislead later updates as mentioned previously. By doing this iteratively, we can obtain a more accurate velocity model.

Study of the TOS impact on FWI sediment update

To understand how sensitive the sediment update was to the TOS error, we designed a series of tests using the BP

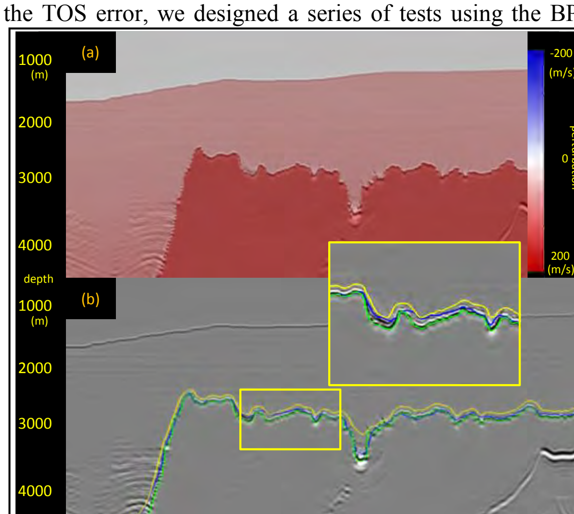

Figure 1: (a) Perturbation between the true salt model and the initial sediment model for salt impact test, (b) three different top of salt (TOS) used for TOS sensitivity test, TOS-1 (yellow), TOS-2 (blue), and TOS-3 (green).

DOI http://dx.doi.org/10.1190/segam2015-5878985.1

2004 benchmark model (Billette and Brandsberg-Dahl, 2005). We chose a section with a complex and rugose TOS. The initial sediment velocity was obtained by scaling the true velocity by 1.05 (Figure 1a). The TOS at different depths—TOS-1, TOS-2, and TOS-3 (Figure 1b)—were used to create salt flood models as FWI initial models. TOS-1 was the TOS interpreted from the sediment flood using the initial sediment model, TOS-3 was the true TOS, and TOS-2 was closer to the true TOS than TOS-1.

When the sediment model was used as the intial model, the velocity update directly above the TOS had a large error (Figure 2a) because the FWI was misled by the large mismatch between the modeled events and real data resulting from the missing salt body. Comparing Figures 2b-2d shows that as the TOS became closer to the true TOS (Figure 2d), the velocity above the TOS gradually approached the true velocity model as the FWI converged. The results demonstrate that TOS accuracy is crucial for the sediment velocity update using FWI. Unfortunately, for real data, the true TOS is not available for the FWI input velocity model.

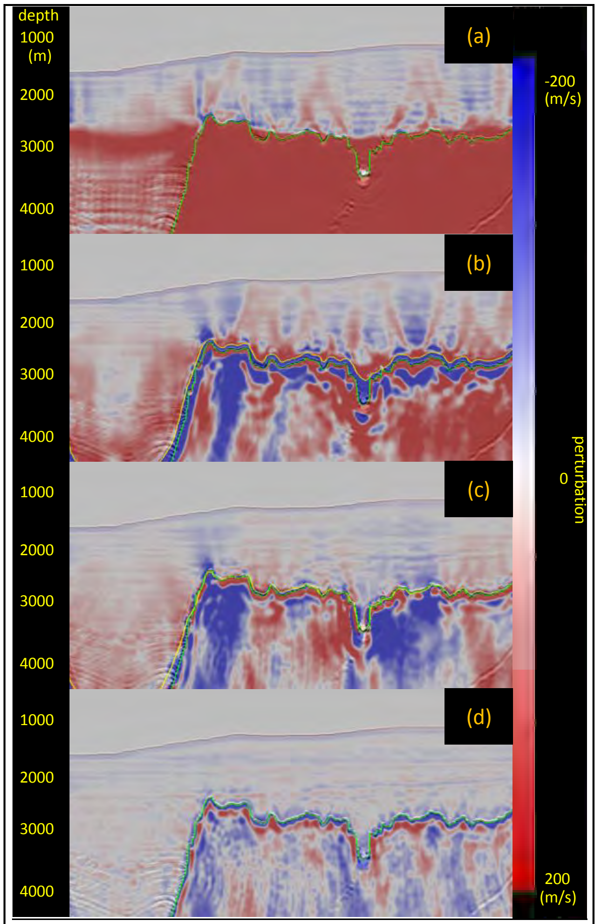

Figure 2: Velocity difference between the full waveform inversion (FWI) output and true model using different FWI initial models: (a) sediment model, (b) salt flood model with TOS-1, (c) salt flood model with TOS-2, and (d) salt flood model with TOS-3. The green line marks the true TOS on all figures, whereas the yellow line marks TOS-1 on (b) and (c).

Iterative FWI workflow

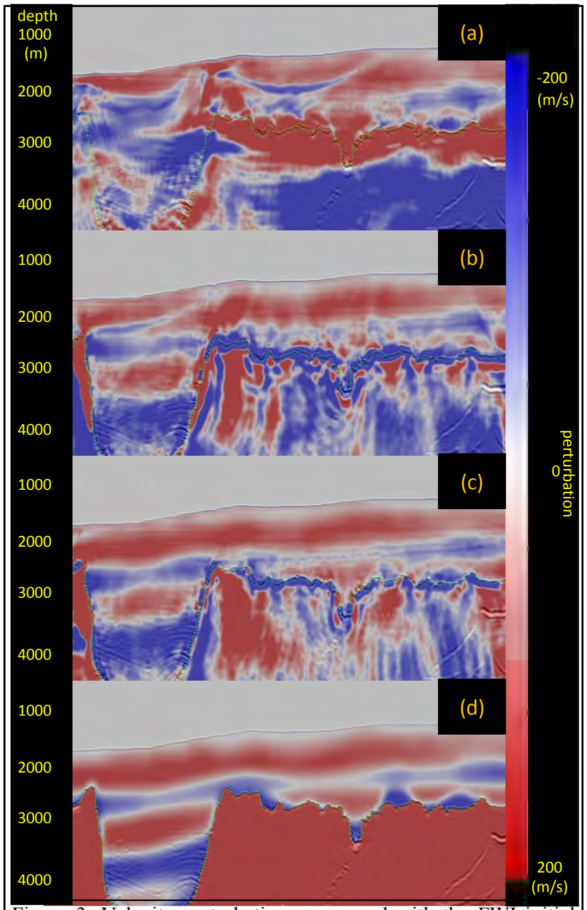

Figure 3: Velocity perturbations compared with the FWI initial model: (a) using the sediment model in FWI, (b) after the first iteration of the iterative FWI workflow, (c) after the second iteration of the iterative FWI workflow, and (d) true perturbation. The green line is the true TOS.

To gradually reduce the error in the sediment velocity update generated by the inaccurate TOS, we propose a workflow that iteratively updates the TOS and the sediment velocity using the following steps:

1. Pick the TOS based on the ray-based tomography sediment velocity model.

DOI http://dx.doi.org/10.1190/segam2015-5878985.1

2. Run FWI with the model generated by inserting the salt into initial sediment velocity model using the picked TOS.
3. Refine the TOS based on the FWI output from Step 2.
4. Iteratively update the sediment velocity and TOS by repeating Steps 2 and 3.

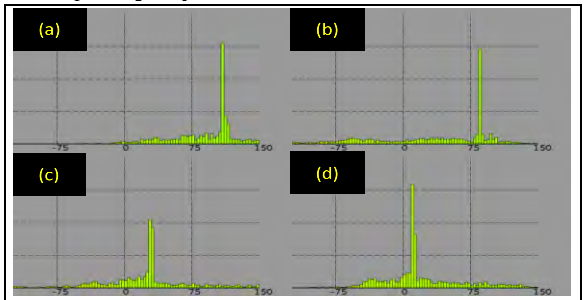

Figure 4: Histogram of the difference between the true TOS and the TOS picked on sediment flood of: (a) initial sediment model, (b) FWI output model using sediment model as initial model, (c) FWI output model using the first iteration of the iterative FWI workflow, and (d) FWI output model using the second iteration of the iterative FWI workflow.

An erroneous TOS interpretation leads to incorrect velocity updates. Hence, after fine-tuning the TOS at each iteration based on the FWI update, the salt is inserted back into the initial sediment model for the next iteration to avoid an incorrect velocity update. As the TOS approaches the true TOS, the velocity update gradually converges to the true velocity model.

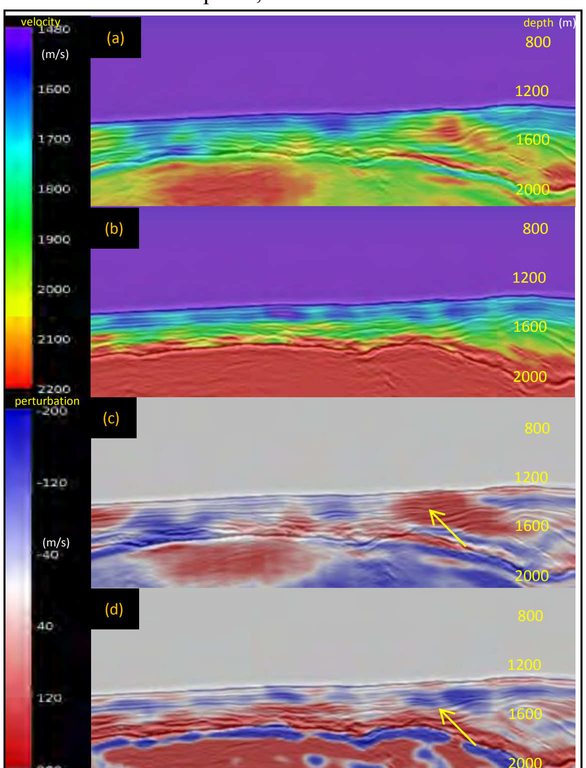

Figure 5: (a) FWI output with sediment model, (b) FWI output with salt model after iterative update, (c) perturbation between FWI output and initial sediment model, and (d) perturbation between iterative FWI output and initial salt flood model.

We also used the BP2004 benchmark model to validate our proposed workflow. The initial sediment model was generated by adding low frequency, ~8-10% random perturbation to the true model in the sediment area (Figure 3d). The FWI update using the initial sediment model provided an incorrect velocity update around the TOS area (Figure 3a), which matched our observations from the TOS impact test (Figure 2). After two iterations of the proposed iterative FWI workflow, the updated velocity was closer to the true velocity (Figure 3b and 3c), and the updated TOS became closer to the true TOS (Figure 4).

Wide azimuth data example

We applied our workflow to a wide azimuth data set from Garden Banks, Gulf of Mexico. The initial sediment model was obtained through ray-tracing tomography. We tested our iterative FWI workflow on the area with shallow TOS (400-900 m below the water bottom) where the sediment velocity update using FWI could be easily misguided by an erroneous TOS.

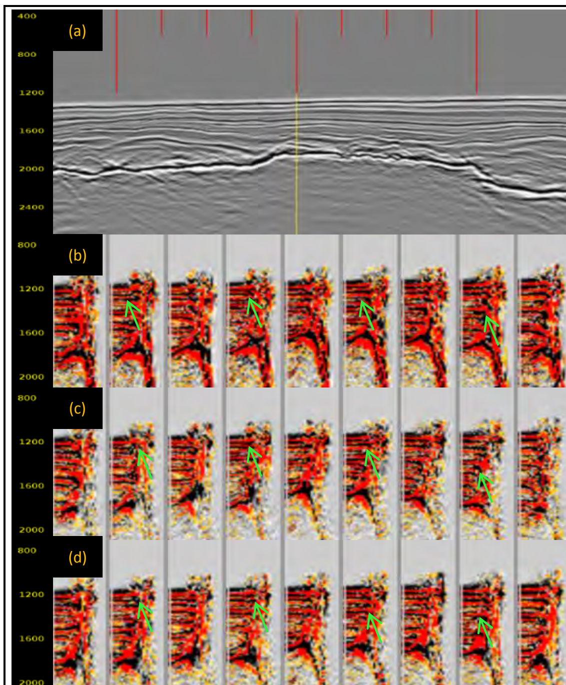

Figure 6: Controlled beam migration results: (a) stack, (b) gathers migrated using initial sediment model, (c) gathers migrated using the FWI update from the sediment model approach, and (d) gathers migrated using FWI update from the FWI iterative workflow. The vertical red lines on (a) indicate the location of the gathers. The green arrows indicate flatness improvement.

DOI http://dx.doi.org/10.1190/segam2015-5878985.1

Similar to the 2D synthetic test, we ran two types of FWI to update the sediment model: (1) using the sediment model as the initial model and (2) using the iterative FWI workflow. The resulting FWI updates were quite different, and we observed opposite polarity perturbations at certain locations (Figure 5). FWI using the iterative workflow provided more detailed updates (Figures 5c and 5d, yellow arrows). We only show the result after two iterative updates; however, internally, the results indicated that the TOS was pushed in the correct direction after each iteration. To validate the updates, we ran controlled beam migration (CBM) to examine the stack and gathers (Figure 6). The flatness of the migrated CBM gathers was deteriorated by the FWI updated model when a sediment model was used as the initial model (Figure 6c). This suggests that the FWI update using the sediment model approach is unreliable. In comparison, the FWI update using the FWI iterative workflow resulted in overall improved TOS events and flatter gathers (Figures 6d).

We also examined the synthetic shot gathers using the velocity model obtained by our workflow. For both supra-salt and TOS events, the synthetic shot gather using the FWI output from the FWI iterative workflow with salt model better matched the real shot gather (Figure 7). To demonstrate the phase difference between the real data and synthetic data, we overlaid the positive amplitude of the synthetic data on the real data (the positive amplitude is shown using red); the better the synthetic matched the real data, the less red color was seen. This again indicated that the FWI update using the FWI iterative workflow with the salt model provided a sensible update.

Conclusion

Synthetic tests involving initial models with different degrees of TOS accuracy indicate that the closer the TOS is to the true TOS, the better the sediment velocity update can be provided by FWI. We present an iterative FWI workflow that provides a better sediment velocity update when compared to FWI using a sediment-only velocity model as input, especially for the velocity directly above the TOS.

While the study improves our understanding of TOS impact on the FWI sediment velocity update, and the proposed iterative FWI workflow provided obvious uplift in the velocity update, the possibly tedious and lengthy process of TOS interpretation during the iterative update could limit the use of this workflow. Also, salt overhangs could pose further challenges that have not been investigated in this study.

Acknowledgements

The authors thank CGG for the permission to publish this work. Special thanks go to Guang Chen, Hongbo Bi, Tao Lin, and Mothi Sabaresen for helpful discussions

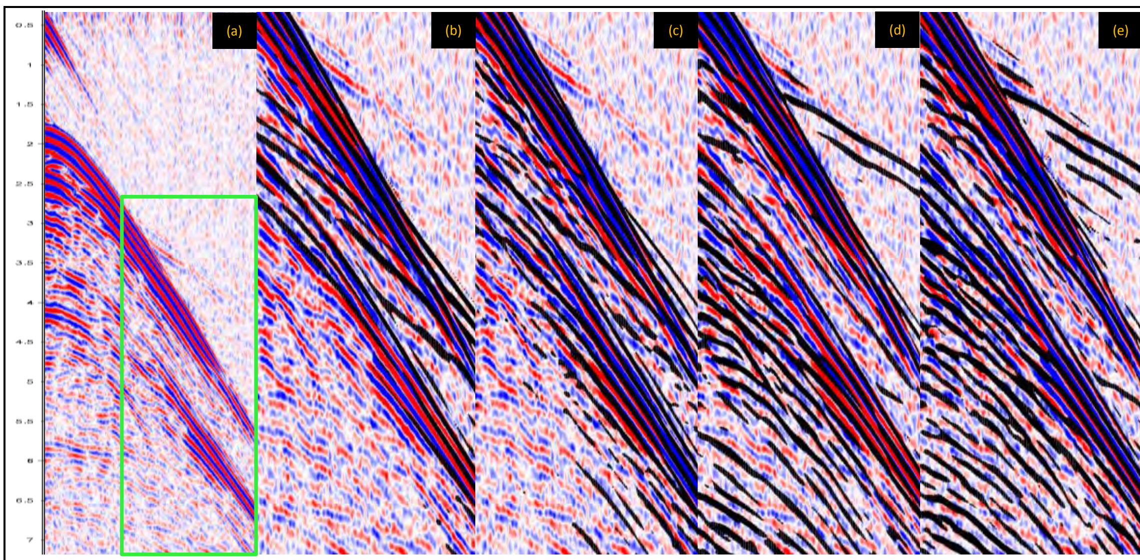

Figure 7: Overlay of synthetic gather (black wiggle) on real data (blue and red). (a) Real data. The green box indicates the location of the zoom-in areas shown in (b)-(e). Synthetic data from (b) sediment initial model. (c) FWI output using sediment model as the initial model, (d) salt flood model, and (d) output of the second iteration of iterative FWI workflow using the salt flood model as the initial model.

DOI http://dx.doi.org/10.1190/segam2015-5878985.1

Reference

Billette, F., and S. Brandsberg-Dahl, 2005, The 2004 BP velocity benchmark: 67th Annual Conference & Exhibition, EAGE, Extended Abstracts, B035.

Chen, C.S., J. Zhang, X. Li, H. Chen, and S. Ji. 2014, Using full waveform inversion to update supra-salt velocity models: a case study in the Gulf of Mexico: 84th Annual International Meeting, SEG, Expanded Abstracts, 26-31.

Kapoor, S., D. Vigh, H. Li, and D. Derharoutian, 2012, Full waveform inversion for detailed velocity model building: 74th Annual Conference & Exhibition, EAGE, Expanded Abstracts.

Lailly, P., 1983, The seismic inverse problem as a sequence of before stack migrations: Conference on Inverse Scattering, Theory and Application, Society of Industrial and Applied Mathematics, Expanded Abstracts, 206-220.

Sirgue, L., and R. G. Pratt, 2004, Efficient waveform inversion and imaging: A strategy for selecting temporal frequencies: Geopysics, 69(1), 231-248.

Tarantola, A., 1984, Inversion of seismic reflection data in the acoustic approximation: Geophysics, 49(8), 1259-1266.

Virieux, J., and S. Operto, 2009, An overview of full waveform inversion in exploration geophysics: Geophysics, 74(6), WCC127-WCC152.

DOI http://dx.doi.org/10.1190/segam2015-5878985.1

EDITED REFERENCES

Note: This reference list is a copyedited version of the reference list submitted by the author. Reference lists for the 2015 SEG Technical Program Expanded Abstracts have been copyedited so that references provided with the online metadata for each paper will achieve a high degree of linking to cited sources that appear on the Web.

REFERENCES

Billette, F., and S. Brandsberg-Dahl, 2005, The 2004 BP velocity benchmark: 67th Annual International Conference and Exhibition, EAGE, Extended Abstracts, B035.

Chen, C. S., J. Zhang, X. Li, H. Chen, and S. Ji, 2014, Using full-waveform inversion to update supra-salt velocity models: A case study in the Gulf of Mexico: 84th Annual International Meeting, SEG, Expanded Abstracts, 26–31, doi: 10.1190/segam2014-0567.1.

Kapoor, S., D. Vigh, H. Li, and D. Derharoutian, 2012, Full-waveform inversion for detailed velocity model building: Presented at the 74th Annual International Conference and Exhibition, EAGE.

Lailly, P., 1983, The seismic inverse problem as a sequence of before stack migrations: Conference on Inverse Scattering, Theory and Application, SIAM, Expanded Abstracts, 206–220.

Sirgue, L., and R. G. Pratt, 2004, Efficient waveform inversion and imaging: A strategy for selecting temporal frequencies: Geophysics, **69**, 231–248. http://dx.doi.org/10.1190/1.1649391.

Tarantola, A., 1984, Inversion of seismic reflection data in the acoustic approximation: Geophysics, **49**, 1259–1266. http://dx.doi.org/10.1190/1.1441754.

Virieux, J., and S. Operto, 2009, An overview of full-waveform inversion in exploration geophysics: Geophysics, **74**, no. 6, WCC1–WCC26. http://dx.doi.org/10.1190/1.3238367.